Journal of Imaging Science and Technology® 64(4): 040403-1–040403-7, 2020.
© Society for Imaging Science and Technology 2020

Fingerprint Quality Assessment based on Texture and Geometric Features

Ching-Han Chen and Chen-Shuo An
Department of Computer Science and Information Engineering, National Central University, Taoyuan, Taiwan, R.O.C.

Ching-Yi Chen
Department of Information and Telecommunications Engineering, Ming Chuan University, Taoyuan, Taiwan, R.O.C.
E-mail: chingyi@mail.mcu.edu.tw

Abstract. *Fingerprint quality assessments are generally used to evaluate the quality of images obtained from fingerprint sensors, and effective fingerprint quality assessment methods are crucial to establishing high-performance biometric identification systems. The use of fingerprint quality assessments helps improve the accuracy of fingerprint registration and user satisfaction. NIST Fingerprint Image Quality (NFIQ) is a popular fingerprint quality assessment algorithm; however, it is unable to provide high-quality assessments for some partial fingerprint images obtained from mobile device sensors. In this study, a hybrid fingerprint assessment framework that integrated texture and geometric features was examined. The final quality assessment values obtained by the framework were higher than those obtained using NFIQ, effectively elevating the performance of existing NFIQ algorithms and expanding its scope of application for different fingerprint images.* © *2020 Society for Imaging Science and Technology.*
[DOI: 10.2352/J.ImagingSci.Technol.2020.64.4.040403]

1. INTRODUCTION

Biometrics is a technology for analyzing biological data or behavioral characteristics for automatically recognizing individuals, which is now becoming an essential component for identification and authentication. Biometric identifiers, considered unique to the individual, are often categorized as physiological versus behavioral characteristics. Physiological characteristics derive from the structural information of the human body, including human fingerprint, face [1, 2], iris [3], and veins [4–6] while behavioral characteristics are based on the behavior of the person. Voice [7], gait [8], and keystroke dynamics [9] are often categorized as behavioral characteristics.

Human fingerprints are a texture formed by raised and sunken skin on the fingers. Each ridge is covered by sweat glands, which cause people to leave marks on objects they touch. The textures on all fingerprints are unique, and no two people in the world have the same fingerprint. Fingerprint minutiae points include where ridges start, end, meet, and branch off. More identifiable minutiae points mean that more samples can be analyzed. Fingerprint matching involves analyzing extracted minutiae points to determine whether they are from the same fingerprints. However, when taking fingerprint images, poor skin surface quality, dirty fingerprint sensors, or uneven contact with sensors can compromise the quality of fingerprint images obtained from sensors, making the subsequent capturing of minutiae points difficult and increasing the risk of identification errors.

Fingerprint quality assessments use mathematical equations to measure fingerprint image quality. By making fingerprint quality assessments, fingerprint identification systems can appropriately reject low-quality fingerprint images and reacquire high quality ones. Because fingerprint quality assessments can, to a certain extent, determine fingerprint matching results, fingerprint image quality can be used as a predictor of biometric identification system performance. In other words, when fingerprint identification systems calculate the quality of input fingerprint images, they can determine whether to accept registering these images or request that users re-input new ones. For building fingerprint databases, this method helps ensure that the fingerprint images in the database are of high quality, complete, and accurate, increasing future fingerprint matching success rates.

Alonso-Fernandez et al. [10] compared several common fingerprint quality assessment algorithms, finding that most algorithms calculated features such as orientation strength in the spatial or the frequency domain of fingerprint images before employing one or multiple feature combinations to obtain the scalar quality values of the images. Features that are commonly recommended consist of orientation certainty level, ridge continuity, ridge–valley structure, and orientation flow [11]. Of all the fingerprint quality assessment methods, the NIST Fingerprint Image Quality (NFIQ) algorithm is a well-known neural network classifier method that uses four block-based features (i.e., ridge orientation flow, ridge orientation certainty, local ridge curvature, and local contrast) and fingerprint image features (e.g., minutiae quality) to create an 11-dimensional quality feature vector [12]. This feature vector is input into a neural network classifier to produce five quality levels that range from poor to excellent quality. However, despite NFIQ producing favorable assessment results when the fingerprint image input is complete, Merkle et al. identified its limitations and asserted that great optimization potential remained for

Received Oct. 24, 2019; accepted for publication Mar. 11, 2020; published online May 14, 2020. Associate Editor: Jia-Shing Sheu.
1062-3701/2020/64(4)/040403/7/$25.00

the image features used by NFIQ to predict image quality [13]. In general, when using NFIQ to make fingerprint quality assessments, systems must calculate the ratio of the fingerprint foregrounds in relation to the entire fingerprint image. This means that when the systems are unable to distinguish between the foreground and the background of the fingerprint images, NFIQ is unable to accurately evaluate the fingerprint image quality. In addition, because some sensors can only record a partial fingerprint image, NFIQ is unable to calculate the correct feature vectors in this situation, resulting in image quality assessment errors.

Because NFIQ is unable to accurately evaluate the quality of incomplete fingerprint images, using it to perform fingerprint identification on mobile devices can yield unfavorable results. In general, most mobile device fingerprint sensors are strictly limited in size; consequently, the captured fingerprint images are usually only a section of the entire fingerprint. Therefore, the use of NFIQ to make fingerprint quality assessments is prone to errors. To solve this problem, an improved fingerprint quality assessment was proposed in this study, where the NFIQ was integrated with the texture features of fingerprint images to build a more robust fingerprint quality assessment method that could more effectively evaluate fingerprint images obtained from a variety of sensors and generate a correct classification of image quality levels. To verify the effectiveness of this method, the devised fingertip quality assessment algorithm was integrated with a FingerCell embedded biometric system [14] to establish a verification platform, which was used to analyze the correlations between fingerprint quality assessment indicators and fingerprint matching performance. The templates used in the experiment included the FVC2006 database [15] and a self-constructed fingerprint database created using different fingerprint sensors.

2. RELATED APPROACHES

2.1 *The NFIQ Method*

Fingerprints are ridges found on the surfaces of fingertips, which help increase friction. For fingerprints to be considered high quality, they should have clear, identifiable texture and features. The details of the ridge and valley structures found on fingerprints are used by automated fingerprint identification systems (AFIS) to perform fingerprint matching. Ridge endpoints and branches are called minutiae points, and all current AFIS are built using minutiae. Minutiae-based AFIS compare the minutiae maps of two fingerprints to generate a matching score. Fingerprint quality directly affects subsequent fingerprint matching results and can even be used as a predictor of such results. NFIQ classifies fingerprint quality into five levels using the following methods [13].

2.1.1 *Generate Image Quality Map*

NFIQ divides the image quality analyzed into quality values ranging from 1 (highest quality) to 5 (lowest quality). A higher fingerprint image quality yields a more pronounced fingerprint matching performance via a matching algorithm. The NIST Biometric Image Software can be used to obtain minutiae points and assess minutiae quality. To analyze fingerprint image quality, the software first divides fingerprint images into several blocks and calculates the direction map, low-contrast map, low-flow map, and high-curve map of each block. Then, the block data are combined to produce a quality map.

(1) Direction map: Direction maps are used to display regions of an image with sufficient ridge structures. To detect the minutiae points of a texture, the fingerprints must be well formed and feature clear ridges.
(2) Low-contrast map: Low-contrast maps are used to segment the background blocks of fingerprint images and mark the blocks with stains or those with unclear fingerprint texture.
(3) Low-flow map: Low-flow maps are used to mark blocks that could not initially be assigned as the dominant ridge flow blocks. Minutiae points detected in such blocks are unreliable.
(4) High-curve map: High-curve maps are used to mark the high-curvature regions of fingerprints. Generally, the minutiae detected in high-curvature regions (particularly those detected in core and delta regions) are unreliable.
(5) Quality map: Low-contrast maps, low-flow maps, and high-curve maps reveal different low-quality regions in images. These map data are integrated into general maps containing five quality levels, which are represented by black, dark gray, medium gray, light gray, and white. In quality maps of fingerprint images, blocks with a quality level of 0 are regarded as the background, whereas those with a quality level of 1 or above are considered effective regions. The percentage of blocks with a quality level of 1–4 occupying all foreground blocks are also called the quality zones, and quality zones with a quality level of 4 represent optimal image quality.

2.1.2 *Assess Minutia Quality*

NFIQ features, created using the NIST Biometric Image Software package, are used in the training of the NFIQ algorithm. NIST minutiae detectors (MINDTCT) can automatically detect the minutiae of fingerprint images input by users, assess the quality of the minutiae, and generate quality maps of the fingerprint images. These data form the basis of NFIQ features. All minutiae detected by the MINDTCT are assigned a quality value of 0.01 to 0.99; low-quality minutiae are detected from low-quality image blocks, whereas high-quality minutiae are detected from high-quality image blocks. In general, minutiae with a quality value of 0.5 or lower are unreliable. Thus, the number of minutiae with a quality value between 0.5 and 0.99 was calculated and used as the basis for assessing image quality.

2.1.3 *Generate NFIQ Features*

NFIQ is a fingerprint quality assessment algorithm based on a neural network classifier. Its input is an 11-dimensional feature vector composed of quality maps and minutiae quality assessments, as listed in Table I.

Table I. NFIQ feature vector description [13].

Item	Feature	Description
1	Foreground	Number of blocks that are quality 1 or better
2	Total of minutia	Number of total minutiae found in the fingerprint
3	Min05	Number of minutiae that have quality 0.5 or better
4	Min06	Number of minutiae that have quality 0.6 or better
5	Min075	Number of minutiae that have quality 0.75 or better
6	Min08	Number of minutiae that have quality 0.8 or better
7	Min09	Number of minutiae that have quality 0.9 or better
8	Quality zone 1	Percentage of the foreground blocks of quality map with quality = 1
9	Quality zone 2	Percentage of the foreground blocks of quality map with quality = 2
10	Quality zone 3	Percentage of the foreground blocks of quality map with quality = 3
11	Quality zone 4	Percentage of the foreground blocks of quality map with quality = 4

2.1.4 *Training the Neural Network*

NFIQ employs machine learning technology to train a three-layer neural network into an image quality classifier with hidden layers that contain 22 neurons. In the present study, data input into the neural network were the 11-dimensional feature vector examined in Table I, whereas the data output were five classes of quality number.

2.2 *Texture Analysis-based Fingerprint Quality Assessment*

2.2.1 *Texture Analysis*

In image quality assessment, texture describes the spatial distribution patterns of the grayscale values of image objects that can reflect object texture such as roughness, smoothness, randomness, and regularity [16, 17]. When images contain numerous similar or identical patterns or basic elements, texture analysis methods may be used to analyze and classify image textures. The purpose of a texture analysis is to identify the appropriate feature value of the image texture, which can then be used to identify image types. In order to improve the performance of fingerprint quality assessment, the study uses the gray-level co-occurrence matrix method to get four more important advanced texture features [17] such as energy, contrast, homogeneity and entropy to be used as the input feature vector of the probabilistic neural network (PNN) classifier. These texture features are as follows.

(1) Energy

Energy is used to measure the uniformity and consistency of an image's texture. The more uniform and consistent the image's texture is, the greater the energy value becomes. By contrast, the more even the element distribution value is, the smaller the energy value becomes. Energy is defined as follows:

$$\text{Energy} = \sum_{i,j} p(i,j)^2, \tag{1}$$

where i and j are the coefficients of co-occurrence matrix, $p(i,j)$ is the co-occurrence times of pairs of the grayscale intensity of the pixel located at ith row and jth column in the co-occurrence matrix, and N is the pixel number of the co-occurrence matrix.

(2) Contrast

Contrast is used to indicate the contrast intensity of an image and its value is proportional to the intensity. Contrast is defined as follows:

$$\text{Contrast} = \sum_{i,j} |i-j|^2 p(i,j). \tag{2}$$

(3) Homogeneity

Homogeneity is the degree to which elements are clustered around the main diagonals in a computed co-occurrence matrix. In a computed co-occurrence matrix, homogeneity value becomes greater when elements with larger values are clustered around the main diagonals. Homogeneity is the exact opposite of contrast. When the contrast of an image decreases, the homogeneity of the image increases. Homogeneity is defined as follows:

$$\text{Homogeneity} = \sum_{i,j} \frac{1}{1-(i-j)^2} p(i,j). \tag{3}$$

(4) Entropy

Entropy, the exact opposite to energy in nature, is used to measure textural complexity or the degree of randomness in the arrangement of elements in a co-occurrence matrix. The wider the grayscale distribution of an image is, the higher the entropy value becomes; conversely, the more concentrated the grayscale distribution of an image is, the lower the entropy value becomes. Entropy is defined as follows:

$$\text{Entropy} = -\sum_{i,j} p(i,j).\log(p(i,j)). \tag{4}$$

2.2.2 *Probabilistic Neural Network*

The single spread PNN was first proposed in Ref. [18]. As can be seen in Figure 1, a PNN is an implementation of a statistical algorithm in which the operations are organized

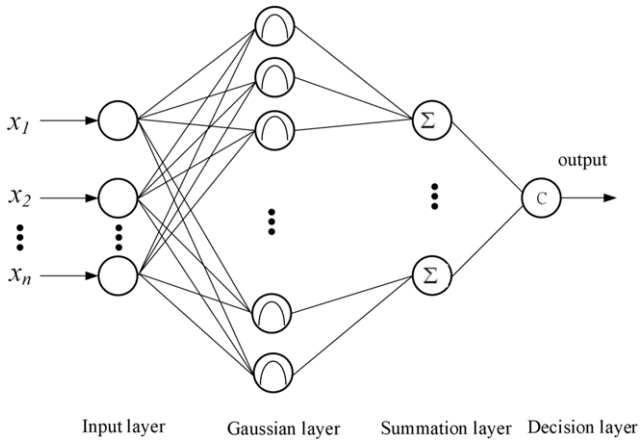


Figure 1. Architecture of a standard probabilistic neural network.

into a multilayered neural network with four layers: input layer, Gaussian layer, summation layer, and decision layer.

The input layer is a linear combination of several multidimensional features. In Gaussian layer, the probability density function (pdf) of each Gaussian neuron is the following form:

$$\varphi_j^i(X) = \frac{1}{(2\pi)^{n/2}\sigma^n} \exp\left(-\frac{(X - Y_j^i)^T(X - Y_j^i)}{2\sigma^2}\right), \quad (5)$$

where n is the length of input vector X, Y_j^i is the n-dimensional jth training example from class C_i, and σ is the smoothing parameter. The calculation of the average of *pdf* for N_i training samples is performed with the following algorithm:

$$P(C_i|X) = \frac{1}{(2\pi)^{n/2}\sigma^n}\left(\frac{1}{N_i}\right)\sum_{j=1}^{N_i}\exp \times\left(-\frac{(X - Y_j^i)^T(X - Y_j^i)}{2\sigma^2}\right), \quad (6)$$

where N_i denotes the total number of samples in class C_i.

The output layer contains one neuron which gives the classification decision for the input vector X in accordance with the Bayes decision rule. The output is calculated as follows:

$$C(X) = \arg\max_{i=1,2,..,m}\left\{\frac{1}{(2\pi)^{n/2}\sigma^n}\left(\frac{1}{N_i}\right)\sum_{j=1}^{N_i}\exp\left(-\frac{(X - Y_j^i)^T(X - Y_j^i)}{2\sigma^2}\right)\right\}, \quad (7)$$

where m is the number of classes presented in the system.

3. DESIGNING THE FINGERPRINT QUALITY ASSESSMENT SYSTEM

The fingerprint quality assessment system introduced in this study comprised three modules: the NFIQ quality assessment module, the texture feature quality assessment module, and the image quality calculation module. IDEF0 from the Integrated Computer-Aided Manufacturing definition (IDEF) was used to produce a hierarchical and modular design for the fingerprint quality assessment system [19]. Structural analyses were conducted to illustrate the relationships between all of the functional modules in the system. Figure 2 illustrates the IDEF0 structure of the proposed fingerprint quality assessment system, where every block was a functional module in the system architecture. A0, the main controller located in the uppermost layer of the system, collected fingerprint images and output their quality values. The A0 system module was further extended into three functional submodules, A1–A3.

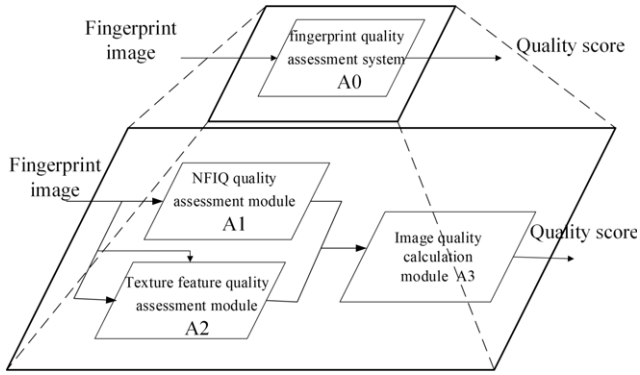


Figure 2. IDEF0 framework of the fingerprint quality assessment system.

(1) A1 module: This module output the NFIQ fingerprint quality assessment results.
(2) A2 module: For this module, the texture factors (e.g., contrast, homogeneity, energy, entropy, and variance) of fingerprint images were first analyzed using the texture analysis module (A21). The calculation results were then sent to the feature vector calculation module (A22) to calculate the mean and variance of each texture factor as well as the fingerprint foreground and background ratio to produce an 11-dimensional feature vector. Finally, the feature vector was input into the PNN decision module (A23) for classification, producing the classification results (Figures 3 and 4).
(3) A3 module: After obtaining the NFIQ and texture feature quality assessment results, the final image quality assessment stage began. The quality calculation module (A3) combined the classification results of the two assessments to produce the final quality values.

4. EXPERIMENTAL RESULTS AND DISCUSSION

4.1 *Fingerprint Image Database*

An experiment was conducted using the FVC2006 database [15] and a new fingerprint database (built using GTS-511E2 fingerprint sensors) [20]. The FVC2006 database, an open access database designated by the international fingerprint verification competition, is a highly respected database in

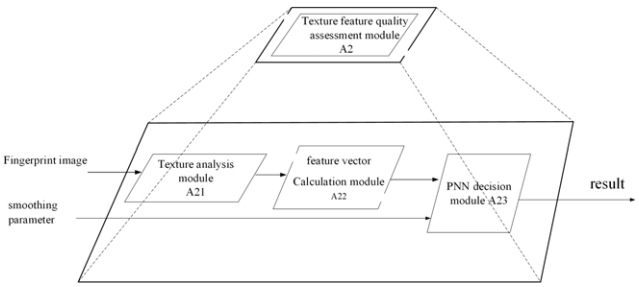


Figure 3. IDEF0 framework of the texture feature quality assessment module.

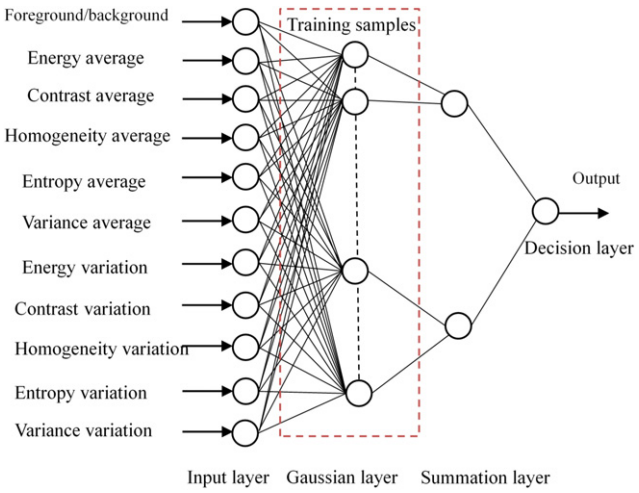


Figure 4. The structure of texture feature quality assessment module.



Figure 5. FVC2006 database based on optical sensor (400 × 560).

both academic and professional circles and is commonly used to test and compare the performance of various fingerprint identification algorithms.

In this study, three subsets of the FVC2006 database were used. Each subset contained 140 fingers and 12 scanned images for each finger, producing a total of 1680 fingerprint images. Together, the three subsets produced a total of 5040 fingerprint images. The images were all in grayscale RAW format. Examples of the fingerprint image templates from these three subsets are shown in Figures 5–7.

In addition to the FVC2006 database, the GTS-511E2 fingerprint sensors were used to capture fingerprint images from 10 fingers; each finger provided 10 fingerprint images for a total of 100 fingerprint images. The image size was 320 × 240, as shown in Figure 8.



Figure 6. FVC2006 database based on thermal sweeping sensor (400 × 560).



Figure 7. FVC2006 database based on SFinGe v3.0 sensor (288 × 384).

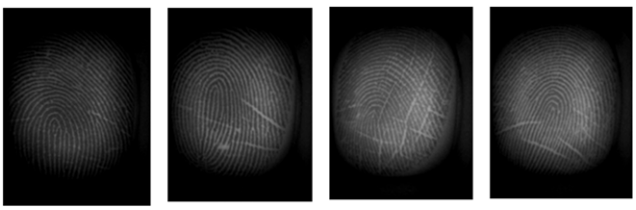


Figure 8. Sample images from the GTS-511E2 fingerprint database.

4.2 *Performance Analysis of the Fingerprint Quality Assessment Framework*

A fingerprint quality assessment system and FingerCell SDK [14] were integrated to produce an experimental verification platform. FingerCell is an embedded biometric system designed for low-power, low-end CPUs that can integrate different hardware and operating system environments quickly and easily to enable developers to rapidly develop operating systems according to their requirements. FingerCell is available for integrators as software development kits (SDK) with FingerCell library for developing a fast and reliable system on embedded platform. It provides functions such as fingerprint template extraction, fingerprint template stitching, and fingerprint template matching. To assess the fingerprint quality classification results, half of the images in the fingerprint database were used as the "match group," and the other half of the images were used as the "test group." When the fingerprint images of the test group were matched with those of the match group, similarity scores were calculated and output. Next, the similarity scores and quality assessment results underwent correlation analysis, and scatter diagrams and trend lines were plotted to verify the performance of the fingerprint quality assessment algorithm. To facilitate the correlation analysis, correlation coefficients were used to demonstrate the degree of correlation between two sets of templates. The correlation coefficients were defined as follows:



Figure 9. Original image.

Assume that two templates (i.e., $x_1, x_2 \ldots, x_n$) and (i.e., $y_1, y_2 \ldots, y_m$) have a template mean of $\bar{x}$ and $\bar{y}$, respectively, and a template standard deviation of S_x and S_y, respectively, with a template covariance of

$$S_{xy} = \frac{1}{n-1} \sum_{i=1}^{n} (x_i - \bar{x}).(y_i - \bar{y}). \tag{8}$$

Then, the correlation coefficient r can be expressed as follows:

$$r = \frac{S_{xy}}{S_x S_y} = \frac{\sum_{i=1}^{n} (x_i - \bar{x})(y_i - \bar{y})}{\sqrt{\sum_{i=1}^{n} (x_i - \bar{x})^2} \sqrt{\sum_{i=1}^{n} (y_i - \bar{y})^2}}. \tag{9}$$

The experiment was conducted using FingerCell, and NFIQ quality indicators of the fingerprint images in the database were calculated, followed by calculating the NFIQ–texture feature quality indicators. In the experiment, texture features were calculated using 9×9 blocks, producing the feature values of contrast, homogeneity, energy, entropy, and variance (Figures 9 and 10(a)–(f)). Next, the means and variances of each feature value, together with the image foreground and background ratio, were calculated to produce feature vectors for input into the PNN decision module. After obtaining the NFIQ quality indicators, texture feature quality indicators, and NFIQ–texture feature quality indicators, FingerCell was used to calculate the similarity scores obtained by matching the fingerprint images with the match group.

After conducting the experiment using the 2520 test images in the FVC2006 database, the fingerprint quality assessment results and fingerprint matching similarity scores were plotted into a scatter diagram and trend lines, as shown in Figure 11(a) and (b).

After conducting the experiment using the 50 test images from the GTS-511E2 database, the fingerprint quality assessment results and fingerprint matching similarity scores were plotted into a scatter diagram and trend lines, as shown in Figure 12(a) and (b).

Table II presents the correlation coefficient analysis of the fingerprint quality assessment and fingerprint matching similarity scores. The correlation coefficients and trend lines revealed that the NFIQ–texture feature fingerprint quality assessment method was more accurate than the NFIQ fingerprint quality assessment.

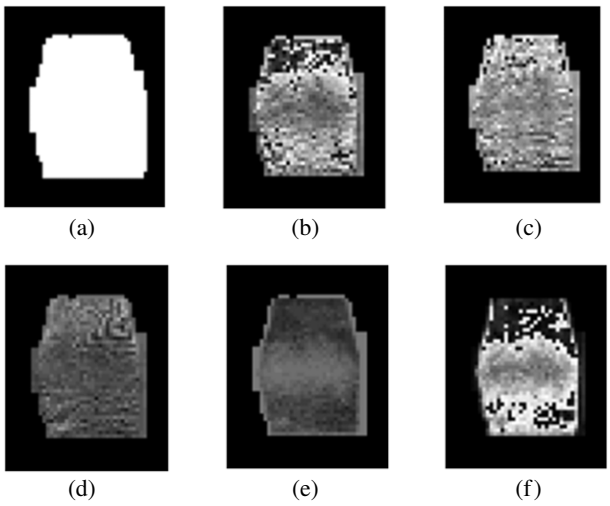


Figure 10. Fingerprint texture feature analysis (a) fingerprint mask image; (b) energy feature image; (c) contrast feature image; (d) homogeneity feature image; (e) entropy feature image; and (f) variance feature image.

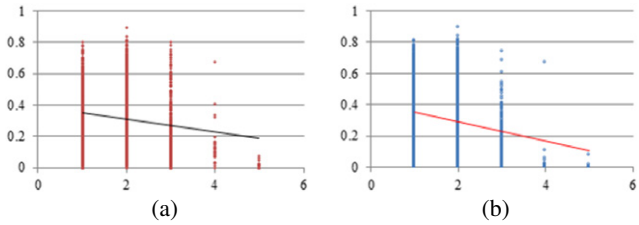


Figure 11. Scatter diagram and trend lines of the fingerprint quality assessment results and fingerprint matching results obtained using the FVC2006 database (a) scatter diagram of the NFIQ image quality assessment and similarity scores; (b) scatter diagram of the NFIQ–texture feature image quality assessment and similarity scores.

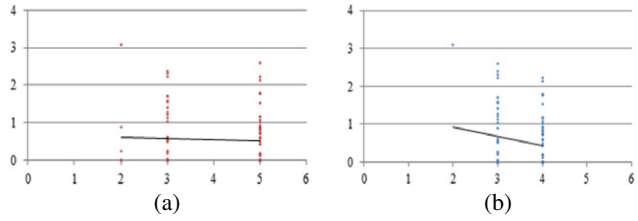


Figure 12. Scatter diagram and trend lines of fingerprint quality assessment results and fingerprint matching results obtained using the GTS-511E2 database (a) scatter diagram of the NFIQ image quality assessment and similarity scores; (b) scatter diagram of the NFIQ–texture feature image quality assessment and similarity scores.

5. CONCLUSION

Fingerprint quality assessments can be used as a predictor for fingerprint matching using AFIS. However, because small size and low cost are the main considerations for fingerprint sensors in mobile devices, the fingerprints extracted by these sensors are usually not the entire fingerprint image but a partial area of the whole fingerprint. Because NFIQ failed

Table II. Correlation coefficient analysis of the fingerprint quality assessment and fingerprint matching similarity scores.

Database	Fingerprint quality assessment method	Correlation coefficient
FVC2006	NFIQ method	0.163370489
	NFIQ–texture feature method	0.212603237
GTS-511E2	NFIQ method	0.043230823
	NFIQ–texture feature method	0.110250568

to exhibit satisfactory assessment capability in its evaluation of such fingerprints, this study proposed to integrate NFIQ with texture feature analysis to improve the NFIQ quality assessment. This proposed method enhanced the quality assessment performance of NFIQ when evaluating incomplete fingerprint images and expanded its scope of application for different types of fingerprint images. In addition, correlation coefficient analysis was conducted according to the obtained image quality assessment results and fingerprint matching similarity scores, and the results verified that the proposed method outperformed the fingerprint image assessment quality of traditional NFIQ.

REFERENCES

[1] Y. F. Liu, J. M. Guo, P. H. Liu, and J. D. Lee, "Panoramic face recognition," IEEE Trans. Circuits Syst. Video Technol. **28**, 1864–1874 (2017).

[2] C. H. Hsia, J. S. Chiang, and C. Y. Lin, "A face detection method for illumination variant condition," Scientia Iranica **22**, 2081–2091 (2015).

[3] J. Chen, F. Shen, D. Z. Chen, and P. J. Flynn, "Iris recognition based on human-interpretable features," IEEE Trans. Inf. Forensics Security **11**, 1476–1485 (2016).

[4] C. H. Hsia, "Improved finger vein pattern method using wavelet-based for real-time personal identification system," J. Imaging Sci. Technol. **26**, 30402 (2018).

[5] C. H. Hsia, "New verification method for finger-vein recognition system," IEEE Sensors J. **18**, 790–797 (2018).

[6] C. H. Hsia, J. M. Guo, and C. S. Wu, "Finger-vein recognition based on parametric-oriented corrections," Multimedia Tools Appl. **76**, 25179–25196 (2017).

[7] I. Bisio, C. Garibotto, A. Grattarola, F. Lavagetto, and A. Sciarrone, "Smart and robust speaker recognition for context-aware in-vehicle applications," IEEE Trans. Veh. Technol. **67**, 8808–8821 (2018).

[8] C. H. Hsia, Y. J. Dai, S. L. Chen, T. L. Lin,, and J. Shen, "A gait sequence analysis for IP camera using a modified LBP," J. Internet Technology **19**, 451–458 (2018).

[9] A. A. Ahmed and I. Traore, "Biometric recognition based on free-text keystroke dynamics," IEEE Trans. Cybernetics **44**, 458–472 (2014).

[10] F. Alonso-Fernandez, J. Fierrez, J. Ortega-Garcia, J. Gonzalez-Rodriguez, H. Fronthaler, K. Kollreider, and J. Bigun, "A comparative study of fingerprint image-quality estimation methods," IEEE Trans. Inform. Forensics Security **2**, 734–743 (2007).

[11] ISO/IEC 29794-4:2010. Information technology – Biometric sample quality – Part 4: Finger image data, Tech. Rep. (2010).

[12] E. Tabassi, C. L. Wilson, and C. I. Watson, "NISTIR 7151 - Fingerprint image quality," Tech. Rep., NIST (2004).

[13] J. Merkle, M. Schwaiger, and M. Breitenstein, "Towards improving the NIST fingerprint image quality (NFIQ) algorithm," *Proc. BIOSIG* (GI, Darmstadt, Germany, 2010), pp. 29–44.

[14] FingerCell SDK, http://www.neurotechnology.com/fingercell.html.

[15] R. Cappelli, M. Ferrara, A. Franco, and D. Maltoni, "Fingerprint verification competition 2006," Biom. Technol. Today **15**, 7–9 (2007).

[16] H. Pang, T. Chen, X. Wang, Z. Chang, S. Shao, and J. Zhao, "Quantitative evaluation methods of skin condition based on texture feature parameters," Saudi J. Biological Sci. **24**, 514–518 (2017).

[17] W. Gomez, W. C. A. Pereira, and A. F. C. Infantosi, "Analysis of co-occurrence texture statistics as a function of gray-level quantization for classifying breast ultrasound," IEEE Trans. Medical Imaging **31**, 1889–1899 (2012).

[18] D. F. Specht, "Probabilistic neural networks and the polynomial adaline as complementary techniques for classification," IEEE Trans. Neural Netw. **1**, 111–121 (1990).

[19] R. J. Mayer, IDEF0 Function Modeling, Air Force Systems Command (1992).

[20] ADH Technology Co. Ltd., http://www.adh-tech.com.tw.